Journal of Molecular Structure 930 (2009) 99–109

Contents lists available at ScienceDirect

Journal of Molecular Structure

journal homepage: www.elsevier.com/locate/molstruc

Revisiting $HgCl_2$: A solution- and solid-state ^{199}Hg NMR and ZORA–DFT computational study

R.E. Taylor [a,*], Colin T. Carver [a], Ross E. Larsen [a], Olga Dmitrenko [b], Shi Bai [b], C. Dybowski [b]

[a] Department of Chemistry and Biochemistry, University of California, Los Angeles, CA 90095-1569, USA
[b] Department of Chemistry and Biochemistry, University of Delaware, Newark, DE 19761-2522, USA

ARTICLE INFO

Article history:
Received 20 March 2009
Received in revised form 29 April 2009
Accepted 29 April 2009
Available online 8 May 2009

Keywords:
Chemical shielding
^{199}Hg NMR
Mercuric chloride
Chemical shift anisotropy
Spin–lattice relaxation
ZORA-DFT

ABSTRACT

The ^{199}Hg chemical-shift tensor of solid $HgCl_2$ was determined from spectra of polycrystalline materials, using static and magic-angle spinning (MAS) techniques at multiple spinning frequencies and field strengths. The chemical-shift tensor of solid $HgCl_2$ is axially symmetric ($\eta = 0$) within experimental error. The ^{199}Hg chemical-shift anisotropy (CSA) of $HgCl_2$ in a frozen solution in dimethylsulfoxide (DMSO) is significantly smaller than that of the solid, implying that the local electronic structure in the solid is different from that of the material in solution. The experimental chemical-shift results (solution and solid state) are compared with those predicted by density functional theory (DFT) calculations using the zeroth-order regular approximation (ZORA) to account for relativistic effects.

^{199}Hg spin–lattice relaxation of $HgCl_2$ dissolved in DMSO is dominated by a CSA mechanism, but a second contribution to relaxation arises from ligand exchange. Relaxation in the solid state is independent of temperature, suggesting relaxation by paramagnetic impurities or defects.

1. Introduction

Mercury is an element known since ancient times. The first emperor of China, Qin Shi Huang, in an effort to achieve immortality, consumed medicines prepared by Taoist priests with cinnabar (HgS) as an ingredient. When he died, he was buried in a tomb at Xian surrounded by his terra cotta soldiers and "rivers of mercury" [1]. Mercury was also used extensively in the process of hatmaking. The inhalation of mercury vapor among workers led, over time, to neurological damage and manifestations such as slurred speech and distorted vision. This apparent mental confusion among members of that profession gave rise to the somewhat clichéd statement, "mad as a hatter" [1].

The interesting and useful features of mercury, frequently given in introductory chemistry texts [2], include the following. As the only metallic element that exists as a liquid at room temperature, it is found in thermometers, sphygmomanometers, electrical switches, and diffusion vacuum pumps. It is used in high-pressure lamps and fluorescent lights as a source of visible and ultraviolet radiation. Its triple point (−38.8344 °C) is a fixed point on the International Temperature Scale 1990. It forms a range of inorganic and organometallic compounds, with many showing biological activity. Although mercury is still commercially useful, toxicity and environmental concerns have restricted the widespread use of mercury and mercury compounds.

The ^{199}Hg isotope is amenable to observation by nuclear magnetic resonance (NMR) spectroscopy. The spin-½ isotope has a natural abundance of 16.8%, and its receptivity relative to ^{13}C at natural abundance is 5.89. The first observation of ^{199}Hg NMR, the resonance of $Hg_2(NO_3)_2$ in aqueous solution, was reported in 1951 [3]. Since that report, the NMR properties of a variety of solutions containing mercury compounds have been investigated. A compilation by Wrackmeyer and Contreras [4] contains a substantial tabulation of solution-state ^{199}Hg chemical shifts.

The ^{199}Hg relaxation properties of neat mercury-containing liquids and mercury compounds dissolved in solvents ranging from alcohols and water to organic liquids have also been examined [5–9]. For smaller molecules such as dimethylmercury, $Hg(CH_3)_2$, and for the Hg^{2+} ion in aqueous solution investigated at the low resonance frequencies encountered when using electromagnets with fields of 2.35 T or less, spin–lattice relaxation is generally dominated by the spin–rotation interaction [4,5]. However, many reports indicate that the chemical-shift anisotropy (CSA) mechanism dominates the ^{199}Hg spin–lattice relaxation in mercury compounds in solution at field strengths greater than 4.7 T [4,6]. Recently, Maliarik and Persson [7] have noted that "despite the number of ^{199}Hg NMR studies undertaken, information on the relaxation behavior of this nucleus is relatively scarce and is mostly related to linear organometallic HgR_2 complexes". Maciel and Borzo [8] reported that the relaxation in mercuric chloride ($HgCl_2$) at 1.4 M in ethanol is exponential, with a ^{199}Hg T_1 of 1.4 s at ambient temperature. A more thorough study of the magnetic-field dependence of spin–lattice relaxation at ambient temperature by Wasylishen et al. [6] demonstrated that

* Corresponding author. Tel.: +1 310 206 2074.
E-mail address: taylor@chem.ucla.edu (R.E. Taylor).

0022-2860/$ - see front matter © 2009 Elsevier B.V. All rights reserved.
doi:10.1016/j.molstruc.2009.04.045

the ^{199}Hg spin–lattice relaxation of $HgCl_2$ in an ethanolic solution is dominated by the CSA relaxation pathway [6]. In principle, measurement of the relaxation time together with an independent measurement or estimate of one parameter should allow specification of the correlation time and the magnitude of the chemical-shift anisotropy. However, they found, over the range of fields and temperatures investigated, that it was not possible to estimate either the correlation time or the chemical-shift anisotropy, as an independent measurement of the other parameter was not available.

Most ^{199}Hg spectra are referenced to the position of the resonance of neat $Hg(CH_3)_2$. Due to both the high toxicity and "revolting" odor of dimethylmercury, spectroscopists have sought more convenient, practical secondary standards. A 1.0 M solution of mercuric chloride, $HgCl_2$, in dimethylsulfoxide (DMSO) has been proposed [9] as an external reference. The resonance position of mercury in this solution is reported to be −1501.6 ppm. As $HgCl_2$ is a Lewis acid [10–12], its structure in electron-donating solvents may be expected to be different from that of the nearly linear Cl–Hg–Cl (bond angle of 178.9°) in the solid material [13], which may result in a chemical shift that is strongly dependent on concentration and/or temperature. The use of DMSO as a solvent in the present study, as opposed to alcohols or water, is meant to eliminate or minimize hydrogen bonding to the chlorine [14].

The observation of ^{199}Hg NMR in a solid material, obtained with cross-polarization and magic-angle spinning (CP/MAS) [15–18], was first reported by Harris and Sebald [15] for mercury acetate. Although their initial NMR study of the acetate was interpreted in terms of a crystal structure having two inequivalent mercury sites, later studies failed to reproduce the peak doubling reported in Ref. [15]. Upon re-examination by other groups, the spectral structure observed for mercury acetate in the original study was determined to be an artifact caused by a deviation of the angle of rotation from the magic angle [17,18]. In their note on the material, Harris and Sebald [15] remarked that the large number of spinning sidebands observed in the spectrum made mercury acetate "far from ideal as a standard" for cross-polarization. Later work provided alternatives to mercury acetate for setting up ^{1}H–^{199}Hg CP/MAS experiments, including $(NEt_4)Na[Hg(CN)_4]$ and $(NBu_4)_2[Hg(SCN)_4]$ [19] as well as $[Hg(DMSO)_6](O_3SCF_3)_2$ [20], whose spectra could be obtained by cross-polarization from protons. In particular, the resonance of mercury in $(NEt_4)Na[Hg(CN)_4]$ is easily detected with cross-polarization, making it a good candidate for optimizing spectroscopic conditions and for use as a secondary standard, with its chemical shift being −434 ppm [19]. Unfortunately, cross-polarization cannot be used in investigations of a species such as $HgCl_2$ because of the lack of protons. Direct polarization techniques, with their limitations, must be used to obtain the spectra.

The purpose of this investigation is to measure and compare the chemical-shift anisotropy of $HgCl_2$ in DMSO solution with that of $HgCl_2$ in the solid state. Such a comparison elucidates structural changes between the two condensed phases. The experimental chemical-shift results are compared with theoretical predictions, providing insights into structure and into strategies for the calculation of chemical shieldings. In addition, an examination of the magnetic-field and temperature dependences of the ^{199}Hg relaxation of $HgCl_2$ elucidates the mechanisms of relaxation in DMSO solution and the solid state. Analysis of the relaxation properties of the solution provides the molecular rotational correlation time as a function of temperature.

2. Experimental and theoretical methods

The ^{199}Hg NMR data were acquired at various magnetic-field strengths using Bruker Avance 300, DSX 300, MSL 300, DRX 400, DRX 500, and AV 600 spectrometers. The solution NMR data were obtained from 0.1, 0.555, and 1.0 M samples of $HgCl_2$ in d_6-DMSO. NMR data on static polycrystalline samples were measured with a standard Bruker X-nucleus wideline probe with a 5-mm solenoid coil. The ^{199}Hg $\pi/2$ pulse width was 3.75 μs. Data for determining the ^{199}Hg spin–lattice relaxation (T_1) in solution were acquired with an inversion-recovery sequence (π–τ–$\pi/2$–acquire) [21]. The significantly longer spin–relaxation times in the solid state were measured by the saturation-recovery technique [21]. Temperature measurements for solution NMR were calibrated with ethylene glycol [22] while the chemical shift of lead nitrate was used to calibrate the solid-state measurements for static [23] and MAS [24–26] experiments.

Simulation of chemical-shift powder patterns for spectra obtained from static samples and from MAS were performed with the solids simulation package ("solaguide") in the TopSpin (Version 2.1) NMR software program from Bruker BioSpin.

Relativistic spin–orbit calculations using the zeroth-order regular approximation combined with density functional theory (ZORA–DFT) were performed using the Amsterdam density functional (ADF) program package [27] and its associated NMR program module [28–31]. The module DIRAC was applied to generate the core potentials for all atom types. Shielding-tensor calculations employed the all-electron ZORA triple-zeta basis with a double set of polarization functions, TZ2P. The local density approximation (LDA) of Vosko, Wilk and Nusair (VWN) [32] was used, augmented with the Becke88–Perdew86 generalized gradient approximation (GGA) (BP86) [33,34].

Calculations were performed on model anionic fragments representing the local structures. The model structures were generated from crystallographic data taken from the Inorganic Crystal Structure Database (ICSD) [35]. To the extent that long-range interactions do not influence the chemical shielding, calculations on fragments should provide an adequate model of the effects of structure on the chemical shielding.

Clusters representing $HgCl_2$ in DMSO solution were optimized at the same level of theory (ZORA–DFT with VWN and BP86), using an implicit DMSO solution simulation based on the conductor-like screening model (COSMO) implemented in ADF [36–39].

3. Results and discussion

3.1. Solution chemical-shift measurements

As noted in the introduction, the accepted chemical shift reference for ^{199}Hg solution NMR spectroscopy is neat dimethylmercury, defined as $\delta = 0$ ppm. However, the toxicity and odor of this compound often lead to the use of secondary references. Sens et al. [9] propose a 1.0 M solution of $HgCl_2$ in DMSO as an external reference, with a chemical shift of −1501.6 ppm at ambient temperature. This solution has been used for establishing the chemical-shift scale in this study.

Sens et al. [9] note several issues related to the use of $HgCl_2$ and other organomercury compounds as external references. These issues include concentration effects, difficulties arising from the dryness of the solvent, pH of the medium, and potential decoupling difficulties. Maliarik and Persson [7] have noted that "the ^{199}Hg chemical shifts can be misleading and non-reproducible unless the temperature is correctly specified or, preferably, the temperature dependence of the chemical shift of the studied species is determined". To address a possible temperature dependence of the secondary standard, the variation with temperature of the ^{199}Hg chemical shift of $HgCl_2$ in d_6-DMSO was carefully evaluated, as shown in Fig. 1. There is a slight temperature dependence of the chemical shift, with the shift reaching a maximum of approxi-

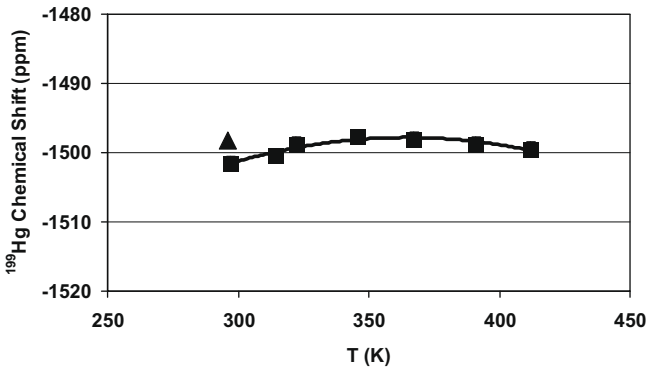

Fig. 1. The temperature dependence of the ^{199}Hg chemical shift of $HgCl_2$ in d_6-DMSO: ■ – 1.0 molar solution; ▲ – 0.10 molar solution.

mately −1498 ± 1 ppm near 350 K. There also appears to be a slight dependence of the chemical shift on concentration at 296–297 K, as can be seen on Fig. 1, the shifts differing by about 3 ppm.

The crystal structure of $HgCl_2$ indicates that, in the solid state, the $HgCl_2$ molecule may be considered linear [13], as shown in Fig. 2. The Cl–Hg–Cl angle is 178.9(5)°, with the two Hg–Cl distances slightly inequivalent at 228.4 and 230.1 pm. The crystal is orthorhombic with a space group of *Pnma*. Each mercury atom has four non-bonded interactions with chlorines on adjacent molecules (with distances ranging from 337 to 348 ppm). By contrast, the structure of mercuric chloride in electron-donating solvents, which can interact with the Lewis acid mercury, may not be linear. In the late 1950s and early 1960s, DMSO became generally available, and the electron-donating functionality of the sulfur–oxygen moiety of sulfoxides was investigated. Several solid-state adducts have been reported. Cotton and Francis [40] isolated a "white crystalline substance" with an elemental analysis corresponding to $(HgCl_2)_2$·DMSO. Selbin et al. [41] used infrared spectroscopy and melting-point determination to characterize $HgCl_2$·DMSO. Biscarini and co-workers have also reported $(HgCl_2)_2$·DMSO [42] and provided a crystal structure for $(HgCl_2)_3$·$(DMSO)_2$ [43]. In this 3:2 adduct, two types of mercury atoms are present: one is somewhat similar to that found for pure $HgCl_2$, but the second forms a dimer of $HgCl_2$·DMSO in which each oxygen is bonded to two mercury atoms.

More recent experimental evidence suggests a $HgCl_2$·$(DMSO)_2$ species in solution [11]. Molar conductance studies indicate that $HgCl_2$ does not dissociate in DMSO [42,44]. ^{199}Hg NMR results are also consistent with a lack of dissociation in solution. For example, in the same solvent, a solvated mercury cation should show the same chemical shift for both the chloride and the acetate, as the mercury atom would be coordinated to the same ligand. However, such behavior is usually observed only with the perchlorate or triflate [7]. That such dissociation does not occur for mercuric chloride is demonstrated in Fig. 3. The resonance position of 0.5 M $HgCl_2$ is −1501.2 ppm, whereas that for 0.5 M $HgBr_2$ is −2058.4 ppm. The separate resonances show that there is no common solvated species present. As a matter of fact, the solvated species, $[Hg(DMSO)_6)]^{2+}$, is known [7,20] and has shifts in solution in the range from −2100 to −2300 ppm [20]. In the solid state, the isotropic peak for this species is at −2313 ppm [20]. Despite the fact that there is no common solvated species, Fig. 3 demonstrates that very fast ligand exchange occurs in the mixture (with an exchange rate on the order of 10^5 at ambient temperature). The middle spectrum results at room temperature when a sample is mixed and placed immediately (on the order of a minute) in the spectrometer.

Evidence from both solution- and solid-state structures indicates two DMSO molecules on one side on the mercury atom in $HgCl_2$, giving a "pseudo-tetrahedral configuration" [45]. Analyses of the Raman and infrared spectroscopy of the stretching vibrational frequencies indicate a Cl–Hg–Cl angle of 162° in DMSO [14], with an earlier solution X-ray diffraction study suggesting ∼165° [46].

There is a decrease in the Hg–Cl bond strength as the bond length increases upon solvation of the mercury atom. In a related

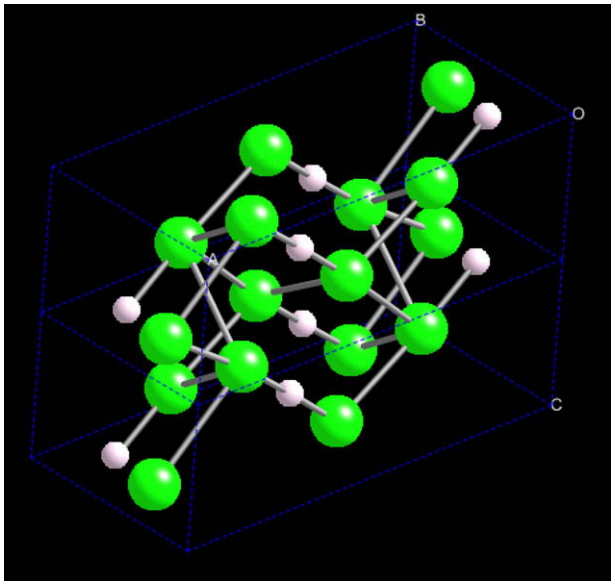

Fig. 2. Two unit cells of $HgCl_2$, showing the nearly linear structure of the Hg bonding environment.

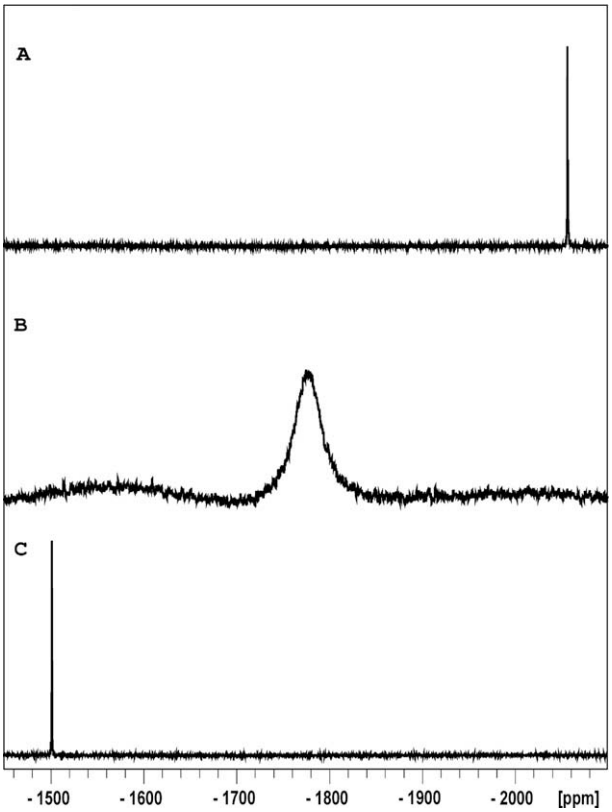

Fig. 3. ^{199}Hg NMR spectra of (A) 0.5 M $HgBr_2$ in d_6-DMSO, (C) 0.5 M $HgCl_2$ in d_6-DMSO, and (B) of the combined 0.5 M $HgBr_2$ and 0.5 M $HgCl_2$ in d_6-DMSO.

chemical system also studied with Raman and infrared spectroscopy, $HgI_2{\cdot}DMSO_2$ has been crystallized from HgI_2 in supersaturated DMSO solutions [45].

3.2. Chemical-shift measurements of the solid and a frozen solution

The ^{199}Hg MAS spectra of polycrystalline $HgCl_2$ (acquired at 7.039 T) as a function of the sample rotation rate are shown in Fig. 4. The smooth lines represent Herzfeld–Berger [47] simulations to extract the principal components of the chemical-shift tensor. These results are compared in Table 1 with previously reported values obtained from spectra of a static sample [48] as well as of one undergoing MAS [49]. Fig. 5 shows the ^{199}Hg variable offset cumulative spectrum (VOCS) of the static solid material, acquired by the technique of Massiot et al. [50], together with a simulation.

The significant result, reflected in Table 1 and Fig. 5, is that the ^{199}Hg CSA is axially symmetric ($\eta = 0$) within experimental error. This finding is materially different from the asymmetry of $\eta = 0.12$ reported by Harris and co-workers [49]. Those authors noted that, for the reported CSA parameters, "accuracy was limited by the high noise levels, and because the spectra required baseline correction. Errors in the shielding tensor parameters were calculated by a published method. They are statistical in nature, and may underestimate the true errors, which would also have systematic and experimental reproducibility contributions". While baseline corrections were applied to the MAS spectra whose results are given in Table 1, this contribution to the error should not affect the VOCS of the static sample obtained with a wideline probe.

The analysis of the ^{199}Hg VOCS shown in Fig. 5(B) warrants further comment. The spectral intensity varies across the resonance in accordance with the anisotropy of the chemical-shift interaction. This results in a lower sensitivity for the upfield δ_{33} component of the spectrum relative to that for δ_{11} and δ_{22}. However, the MAS data provide an additional constraint on the simulation, as the isotropic value from the MAS spectrum is one-third of the trace of the chemical shift tensor, i.e., $(\delta_{11} + \delta_{22} + \delta_{33})/3$. While Grishin et al. [48] were unable to resolve this spectral feature in their ^{199}Hg wideline spectrum of solid $HgCl_2$, they did obtain a value for the δ_{33} component by using the isotropic shift as measured in solution. As demonstrated above, the reported isotropic shift of $HgCl_2$ in d_6-DMSO differs significantly from that of solid $HgCl_2$ as given in Table 1. As a result, the literature values from Grishin et al. [48] for the CSA differ from those reported here.

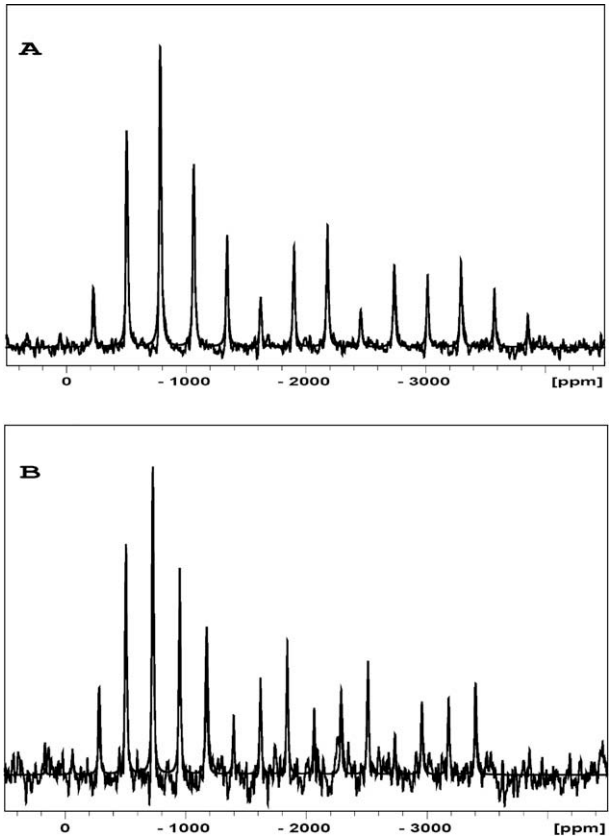

Fig. 4. ^{199}Hg MAS spectra of $HgCl_2$ obtained with the sample being spun at (A) 15 kHz and (B) 12 kHz about the magic angle. The smooth line in each is the simulation used to extract the principal components of the chemical shift tensor. The isotropic shift is −1625 ppm.

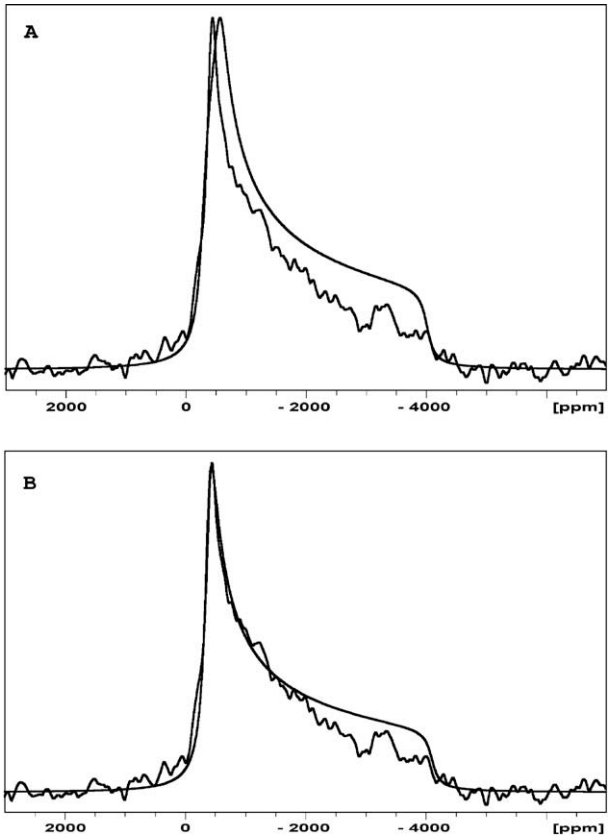

Fig. 5. The same ^{199}Hg VOCS of $HgCl_2$ is shown in (A) and (B). The smooth line in (A) is a simulation using the values of the principal components of the chemical-shift tensor reported by Bowmaker et al. [49]. The isotropic shift is −1625 ppm. The smooth line in (B) is a fitted simulation with the extracted parameters listed in Table 1.

The ^{199}Hg VOCS of a flash-frozen 1 M solution of $HgCl_2$ in d_6-DMSO at 273 K is shown in Fig. 6. The signal-to-noise ratio of this spectrum is significantly lower than that of the polycrystalline solid of Fig. 5. Comparison of the concentration of the solution with that of the density of the solid indicates that the number of mercury atoms is down by a factor of about 20 in the frozen sample. The smooth line in Fig. 6 is a simulated chemical-shift powder pattern with $\delta_{iso} = -1291$ ppm, $\zeta_{cs} = -1400$ ppm and $\eta = 0.1$ (or alternatively $\delta_{11} = -521$ ppm, $\delta_{22} = -661$ ppm, and $\delta_{33} = -2691$ ppm).[1] The experimental spectrum in Fig. 6 for the frozen 1 M $HgCl_2$ in d_6-DMSO

[1] Care must be exercised in referring to the chemical shift anisotropy, as there are two commonly accepted definitions [51]: $\varsigma = \delta_{33} - \delta_{iso}$ and $\Delta\delta = \delta_{33} - \frac{1}{2}(\delta_{11} + \delta_{22}) = \frac{3}{2}\varsigma$. In this article, while reference to the Haeberlen, Mehring, and the "Maryland" notations [51] is given as a convenience to the reader, the principal components of the chemical-shielding tensor are always be stated explicitly to avoid confusion among the different notations.

Table 1
^{199}Hg chemical shift tensor parameters of solid $HgCl_2$.

Experiment	δ_{11}	δ_{22}	δ_{33}	δ_{iso}	ζ_{csa}[d]	η[e]	Ω[f]	κ[g]
15 kHz MAS[a]	−401	−442	−4034	−1625	−2409	0.02	3633	0.98
12 kHz MAS[a]	−413	−413	−4050	−1625	−2425	0.00	3637	1.00
11.0 kHz MAS[b]	−421	−421	−4028	−1623	−2405	0.00	3607	1.00
8.3 kHz MAS[b]	−424	−427	−4009	−1620	−2389	0.00	3585	1.00
Static[a]	−385	−385	−4104	−1625	−2479	0.00	3719	1.00
Average	−409	−418	−4045	−1624	−2421	0.004	3636	1.00
6.6–13.2 kHz, MAS (Harris)[c]	−282	−573	−4019	−1625	−2394	0.12	3737	0.84
Theory								
ZORA–DFT (large cluster)	−5	−73	−4332	−1470	−2862	0.05	4327	0.97
ZORA–DFT (small cluster)	148	65	−4663	−1483	−3180	0.03	4810	0.97

[a] Chemical shifts referenced to neat dimethylmercury by use of 1 M $HgCl_2$ in d_6-DMSO as a secondary reference assigned as −1501.6 ppm (Ref. [9]).
[b] Chemical shifts referenced to neat dimethylmercury by use of $[N(Et)_4]Na[Hg(CN)_4]$ as a secondary reference assigned as −434 ppm (Ref. [19]).
[c] From Ref. [49].
[d] $\zeta_{csa} = \delta_{33} - \delta_{iso}$.
[e] $\eta = (\delta_{22} - \delta_{11})/\zeta_{csa}$.
[f] $\Omega = |\delta_{33} - \delta_{11}|$.
[g] $\kappa = 3(\delta_{22} - \delta_{iso})/\Omega$.

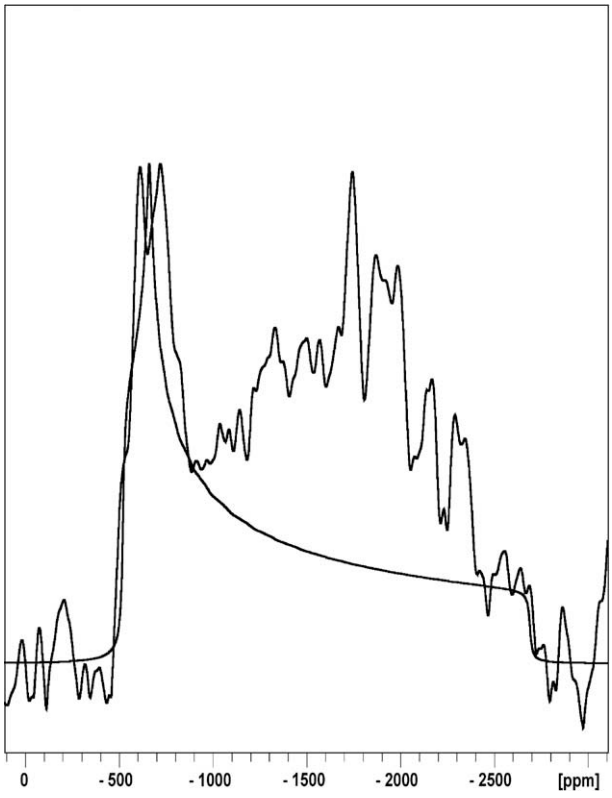

Fig. 6. ^{199}Hg VOCS of a frozen 1 M $HgCl_2$ in d_6-DMSO solution at 273 K. The smooth line is a simulated CSA powder pattern with $\delta_{iso} = -1291$ ppm, $\delta_{csa} = -1400$ ppm and $\eta = 0.1$.

solution indicates the presence of at least one other species, with a resonance band in the region around −1800 ppm. Neither species has the spectral characteristics of solid $HgCl_2$, i.e., a precipitate.

In contrast to the flash-frozen solution, the ^{199}Hg high-resolution solution data indicate only a single species (Figure S1 in the Supporting Information). The observed line shape is well described by a single Lorentzian with a full width at half height of 22.1 Hz.

3.3. Relaxation of $HgCl_2$ in DMSO solutions

A second bit of evidence that there is, on the NMR time scale, but a single species in solution is the relaxation behavior. The spin–lattice relaxation data (Figure S2 in the Supporting Information) are well fit by a single exponential, yielding a T_1 of 34.3 ms, measured at a field of 14.095 T and a temperature of 296 K. The dependence of the ^{199}Hg spin–lattice relaxation rate constant ($1/T_1$) on the square of the Larmor frequency (or, equivalently, the magnetic-field) for $HgCl_2$ in d_6-DMSO at 297 K in Fig. 7 demonstrates that, at these magnetic-field strengths, the CSA mechanism dominates the relaxation behavior. For this mechanism, the relaxation rate constant is given as [21]

$$R_1(\mathrm{CSA}) = 1/T_1(\mathrm{CSA}) = \frac{1}{15}\gamma^2 B_0^2(\sigma_{\|} - \sigma_{\perp})^2 \frac{2\tau_c}{1+\omega^2\tau_c^2}, \quad (1)$$

where γ is the magnetogyric ratio; B_0 is the magnetic induction; $\sigma_{\|}$ and $\sigma_{\perp}$ refer to the shielding when the magnetic-field is parallel and perpendicular to the symmetry axis of the tensor; ω is the resonance frequency; and τ_c is the rotational correlation time. As shown in Fig. 8, the ^{199}Hg relaxation rate ($1/T_1$) of $HgCl_2$ in d_6-DMSO decreases with increasing temperature, which excludes the possibility of relaxation due to the spin–rotation relaxation mechanism [21].

Measurement of the ^{199}Hg spin–lattice relaxation time as a function of field only provides the product of the anisotropy with

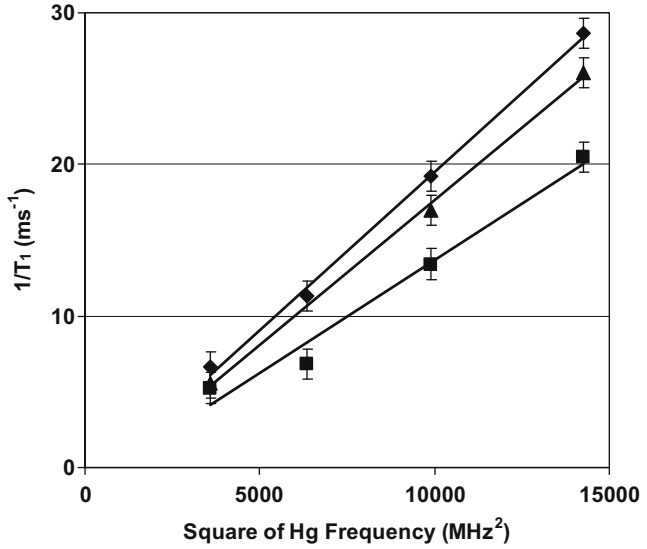

Fig. 7. The Larmor-frequency (magnetic-field) dependence of the ^{199}Hg relaxation rate ($1/T_1$) for three different concentrations of $HgCl_2$ in d_6-DMSO at 297 K. ♦ – 1.0 molar; ▲ – 0.555 molar; ■ – 0.10 molar.

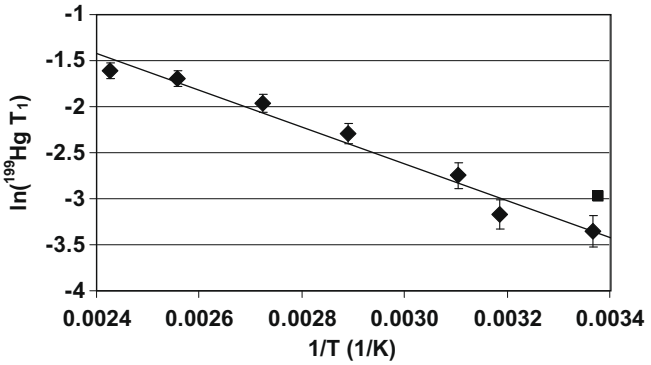

Fig. 8. ^{199}Hg spin–lattice relaxation times in the laboratory frame (T_1) for $HgCl_2$ in d_6-DMSO as a function of inverse temperature: ♦ – 1.0 molar; ■ – 0.1 molar.

the correlation time. The challenge is to measure one of these factors independently. For example, in a study of several mercury compounds, Wasylishen et al. [6] were unable to estimate the anisotropy and correlation time for $HgCl_2$ in solution, although they reported a correlation time of 40.8 ps for $Hg(CN)_2$ and 30.8 ps for $Hg(C_6H_5)_2$ in solution. For further comparison, Maliarik and Persson [7] reported correlation times of various mercury(II) solvates, such as 24 ps for $[Hg(H_2O)_6]^{2+}$ and 254 ps for $[Hg(OS(CH_3)_2)_6]^{2+}$.

The temperature dependence of the ^{199}Hg T_1 for $HgCl_2$ in Fig. 8 is consistent with a simple thermally activated process inducing relaxation. In the extreme-narrowing limit ($\omega\tau_c << 1$) of Eq. (1) appropriate to a solution, the data of Fig. 8 yield an activation energy of 16.6 ± 1.2 kJ/mol. The value of T_1 at ambient temperature (0.15 s) in a magnetic-field of 7.04295 T and an anisotropy of $(\sigma_{11} - \sigma_{\perp}) = [\sigma_{33} - (\sigma_{11} + \sigma_{22})/2] = 2100$ ppm estimated from the spectrum of the frozen solution at 273 K give a determination of the correlation time of $\tau_c = 99.8$ ps under those conditions. The average correlation time for the four ambient-temperature spin–lattice relaxation times of the 1 M solution obtained at the four magnetic fields, as shown in Fig. 7, is 106 ± 7 ps.

Unlike the approach described above for determining the correlation time by measuring the anisotropy in a frozen solution, the usual method [7] for determining the correlation time involves measurement of the viscosity. The correlation time is determined from the Stokes–Einstein equation [52]

$$\tau_c = \frac{V\eta}{kT} \tag{2}$$

where η is the viscosity, k is Boltzmann's constant, T is the absolute temperature, and V is the volume of the molecule (the calculation of which requires the assumption of a model). For some molecules, the presence of other NMR-active atoms allows an independent determination of the correlation time. For example, Gillies et al. [53] *assumed* a linear geometry for $Hg(C_6H_5)_2$ in solution and used variable temperature ^{13}C T_1 measurements for the carbon nucleus at the *para* position to determine a correlation time of 50 ps for motion perpendicular to the molecular axis. With this value, they inferred an anisotropy of 6800 ppm from the ^{199}Hg relaxation data. For $Hg(CN)_2$ in solution, Wasylishen et al. [6] obtained a correlation time of 40.8 ps from the width at half height of the ^{14}N resonance. However, they were unable to observe either the ^{35}Cl or ^{37}Cl resonance of $HgCl_2$ in solution, which prevented them from estimating either the correlation time or the anisotropy.

The correlation time may be estimated from the viscosities of the solutions at room temperature, which are tabulated in Table 2, in accordance with Eq. (2). Using the bond distances from the X-ray structure [13] of 228.4 and 230.1 pm and a van der Waals radius

Table 2
Viscosities used for calculation of correlation times.

Sample	Temperature (°C)	Density (g/cc)	Absolute viscosity (cP)
DMSO	25	1.0989	2.02
0.555 M $HgCl_2$ in DMSO	25	1.2275	2.62

[54] of 175 pm for chlorine, a calculation shows that a linear $HgCl_2$ molecule hydrodynamically sweeps out a spherical volume of 276.6×10^{-30} m^3. The measured viscosity of 2.62 cP for the 0.555 M solution predicts, via Eq. (2), a correlation time of 176 ps. Alternatively, a volume of 305.3×10^{-30} m^3 can be calculated on the basis of atomic spheres from the van der Waals radii [54] of the atoms for $HgCl_2{\cdot}(DMSO)_2$, yielding a correlation time of 194 ps. These estimates of the correlation time compare well with the value of 106 ± 7 ps obtained from the spin–lattice relaxation time in combination with the anisotropy from the frozen solution.

The Stokes–Einstein equation was originally derived for a solute particle of radius r_s moving through "a homogenous, continuous, incompressible fluid" [55], implying that, on a molecular level, the radius of the solute is much greater than the radius of the solvent. Kivelson and co-workers [55] demonstrated, via a molecular-statistical derivation, that the relationship holds for a solute with a radius equal to or greater than that of the solvent, in agreement with experimental observation. This suggests that the calculation with the Stokes–Einstein relation is appropriate in this case, even though the volume of DMSO on the basis of van der Waals radii, 123.2×10^{-30} m^3, is not much smaller than that found for the $HgCl_2{\cdot}(DMSO)_2$. As noted above, a model must be invoked to calculate V for use in the Stokes–Einstein relationship. Kurnikova et al. [56] note that "it is not obvious how to treat the solute solvent frictional coupling when the solute displays complex formation with the solvent," leading to various models for defining a hydrodynamic volume for the solute molecule. The assumption of a slightly smaller molecular volume than either of those noted above would have brought this calculation into closer agreement with the spin–lattice relaxation-derived correlation time.

Strictly speaking, the chemical-shift interaction responsible for the relaxation of $HgCl_2$ dissolved in d_6-DMSO is not likely to be axially symmetric, as reflected in Eq. (1). After all, the experimental data [14,46] suggest a Cl–Hg–Cl bond angle of about 165° in DMSO solution, rather than the near-linear bond in the solid. In the general case of chemical-shift-induced relaxation in "asymmetric top" molecules, three rotational correlation times are required to specify the random dynamics [57]. These three correlation times are often assumed to be identical because the motion is effectively isotropic. For example, in the general case of relaxation by modulation of an asymmetric chemical-shift tensor, Abragam considers only the result for fast isotropic random motion [58]. In the work presented here, the relaxation data are analyzed with Eq. (1), assuming an approximately axially symmetric chemical-shift tensor. The simulation of the spectrum of the frozen solution (Fig. 6) suggests that this is a reasonable approximation.

The ^{199}Hg spin–lattice relaxation data of Fig. 9 indicate a dependence on the concentration of $HgCl_2$ in d_6-DMSO, with the dependence being approximately linear. Without cross-correlation effects, the spin–lattice relaxation rate may be written as the sum of rates of different contributions as

$$R_1(\mathrm{OBS}) = R_1(\mathrm{CSA}) + R_1(\mathrm{2nd}) = 1/T_1(\mathrm{CSA}) + 1/T_1(\mathrm{2nd}) \tag{3}$$

where R_1(OBS) is the observed experimental relaxation rate, R_1(CSA) is the contribution to the relaxation rate due to chemical-shift-anisotropy mechanism, and R_1(2nd) is the relaxation due to

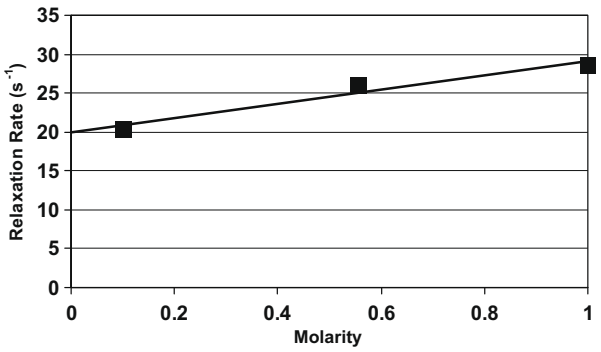

Fig. 9. ^{199}Hg spin–lattice relaxation rate in the laboratory frame (T_1^{-1}) of $HgCl_2$ in d_6-DMSO as a function of concentration.

an intermolecular interaction. The intermolecular interaction is assumed to be linear in concentration. The intercept of the plot in Fig. 9 is the contribution from the intramolecular chemical-shift-anisotropy mechanism.

The extrapolated chemical-shift-anisotropy contribution to the relaxation rate can be used to calculate the rotational correlation time from Eq. (1). This calculation predicts a correlation time from the spin–lattice relaxation time of 69 ps. This value is comparable in magnitude to the correlation times observed by Gillies et al. [53] and by Wasylishen et al. [6] for other mercury-containing materials.

Fig. 3 provides evidence of very fast ligand exchange for $HgCl_2$ in DMSO. The question arises as to whether or not such exchange is fast enough to affect the spin–lattice relaxation of the ^{199}Hg nuclei. Shriver and Atkins [59] have noted that "complexes of low oxidation number d^{10} ions (Zn^{2+}, Cd^{2+}, and Hg^{2+}) are highly labile," with typical exchange times on the order of "1 ns at room temperature." Huheey et al. [60] have noted that fast exchange of water gives first-order rate constants "on the order of 10^8 s^{-1}, which approaches the maximum possible rate constant (calculated to be 10^9–10^{11} s^{-1} for a diffusion controlled reaction)."

In the present case of $HgCl_2$ in DMSO, conductivity measurements and ^{199}Hg NMR show that no ionization occurs. An estimation for the exchange time for the labile chlorine in the diffusion-limited case can be made by generalizing a method used to find mean free paths in gas-phase transport theory [61]. In brief, the Einstein–Smoluchowski equation [52] relates the diffusion coefficient to the parameters of a random walk. If the distance traveled by a random walker in each step is l_0, and the time for each step is t_{step}, then

$$D = \frac{l_0^2}{2t_{step}} \tag{4}$$

The random walker traces out a path of length $n*l_0$ in a time $T = n * t_{step}$, and thus sweeps out an encounter volume $n*l_0*A$, where A is the reaction cross-section for the diffusing molecule. Combining these relations, eliminating t_{step}, and noting that on average the diffuser will meet another $HgCl_2$ molecule when the encounter volume equals the inverse of the $HgCl_2$ concentration, one finds an average exchange time of

$$T = \frac{l_0}{2AcD} \tag{5}$$

where c is the solute concentration. The step length, which is the distance a diffusing particle moves during the velocity decorrelation time, must be of the order the interparticle spacing in solution, say $l_0 \sim 10^{-10}$ m. Similarly, the reaction cross-section must have a value of molecular dimensions, e.g., $A \sim \pi * (2 \times 10^{-10}\ \mathrm{m})^2$. Finally, the self-diffusion coefficient of DMSO at 25 °C, $D = 0.730 \times 10^{-9}$ m^2/s [62], is used as an estimate of the $HgCl_2$ diffusion coefficient, as both the short spin–lattice and spin–spin relaxation times of the ^{199}Hg nucleus in 1 M $HgCl_2$ solutions in DMSO preclude the direct measurement of the $HgCl_2$ by ^{199}Hg pulsed-field-gradient diffusion experiments. Inserting these estimated values into Eq. (5), an exchange time of ~1 ns is obtained for a 1 M solution of $HgCl_2$. Given this lability of mercury ligands, it seems reasonable to assume that the DMSO molecules also exchange, probably on an even faster time scale [60] as DMSO is the solvent medium.

The time scales for the various processes should be kept in mind. The study and modeling of vibrational relaxation [63] indicate molecular collisions occur on the order of picoseconds in liquids. The rotational correlation times derived from the NMR relaxation measurements are on the order of 100 ps, in good agreement with "the rotational relaxation of solute particles of a few hundred cubic angstroms in volume [that] occurs on time scales of 10–100 ps," as measured in ultrafast laser studies [64]. Finally, the chlorine atoms exchange at a rate on the order of 1 per nanosecond. Given the magnetic moments of ^{35,37}Cl, it is important to realize that this exchange is fast enough (compared with the inverse of the ^{199}Hg Larmor frequency) to affect the spin–lattice relaxation of the ^{199}Hg significantly. This relaxation effect arises from the fluctuating magnetic-field due to the time dependence of either the dipolar interaction between the mercury and the chlorine nuclei or scalar interaction [21]. This intermolecular exchange is, most likely, the origin of the intermolecular relaxation mechanism of the mercury nuclei.

In contrast to the ^{199}Hg relaxation behavior in solution, the ^{199}Hg spin–lattice relaxation time in the solid measured at 7.039 T is 51 s and is independent of temperature over range from 293 to 400 K. This behavior is consistent with relaxation by paramagnetic impurities or defects.

3.4. Theoretical prediction of chemical shielding

Electronic structure calculations may be used to determine the NMR *chemical shielding* [65–67]. The *chemical shift*, δ, is the difference in shielding between the nucleus in the species under investigation, σ_s, and the shielding of the same nucleus in a reference compound, σ_{ref}. It is determined by the following formula:

$$\delta_i = \frac{\sigma_{ref} - \sigma_i}{1 - \sigma_{ref}} \tag{6}$$

For lighter elements, the calculations are straightforward and can be performed with several commercially available programs. Accurate calculations for heavy atoms like mercury require that one account for the relativistic nature of the electrons. Nakatsuji et al. [65] used a spin–orbit-unrestricted-Hartree–Fock approach to perform the first *ab initio* calculations, including relativistic effects, to determine the isotropic ^{199}Hg shielding in the mercury dihalides. They concluded that the inclusion of terms such as the spin–orbit term was essential to explain, even qualitatively, trends in chemical shielding.

The ZORA–DFT technique, unlike that of Nakatsuji et al. [65], recasts the Hamiltonian for the one-electron Dirac equation as a Hermitian operator that does not suffer from variational instabilities in the core region of a heavy atom [66]. The ZORA–DFT chemical shielding is the sum of three terms: a paramagnetic contribution, a diamagnetic contribution, and a spin–orbit (or Fermi-Dirac) contribution. Importantly for the interpretation of relaxation measurements, the ZORA–DFT–NMR shielding calculation gives the principal elements of the chemical-shielding tensor. For example, Wolff et al. [66] used the ZORA–DFT method to account for relativistic effects in the calculation of *isotropic* ^{199}Hg NMR chemical shifts of the dihalides and in clusters meant to simulate the effects of solvents, such as tetrahydrofuran (THF), methanol, DMSO, and

pyridine, on chemical shielding of the dihalides in solution. Based on their calculations, they conclude that "it is reasonable to assume that for the solvents THF, DMSO, and pyridine, the mercury halides are closest to their gas phase nature in THF, and furthest from their gas phase nature in pyridine." In later reports, Jokisaari et al. [67,68] gave the results of calculations, also from ZORA–DFT calculations, of the isotropic shielding, the anisotropy of the chemical shielding, and ^{199}Hg–^{13}C spin–spin couplings in the methylmercury halides. For all of the systems they considered, the measured anisotropy of the chemical shielding was quite large, ranging from 4800 to 7300 ppm. The ZORA–DFT calculations also gave large values for the anisotropy, but consistently overestimated the halide chemical-shielding anisotropies by over a 1000 ppm. The calculations correctly predicted the trend of the anisotropy with halide ion. However, the calculated isotropic shift with respect to dimethylmercury was consistently less shielded (often by 100–200 ppm) than the measured shift. These results reflect the state of the art of this type of calculation.

Wolff et al. [66] report that a change in the bond length of 1 pm in $HgCl_2$ results in a change of approximately 50 ppm for the calculated isotropic shifts. They also report a change of approximately 100 ppm for every 10° change in the Cl–Hg–Cl bond angle. Therefore, calculated ^{199}Hg chemical shifts within a few 100 ppm are quite good, given that the ^{199}Hg chemical shift range is over 5000 ppm [65]. Similarly, Autschbach and Ziegler [69] found substantial solvent effects on the ^{199}Hg–^{13}C spin–spin coupling constants of methyl mercury halides.

The ZORA–DFT technique is used in this study to calculate the ^{199}Hg NMR shieldings of solid $HgCl_2$ and of $HgCl_2$ complexed with DMSO to represent structures in the solid state and those that may exist in solution (with fully optimized structures for the solution models). The models were clusters of varying size, to emphasize the fact that the molecules do not exist in isolation. The results for clusters of $HgCl_2$ of different size provide an indication of the importance of short- and long-range interactions.

The chemical shielding of dimethylmercury, the standard reference material in ^{199}Hg NMR, was examined by calculations on clusters of various sizes. Table 3 reports the contributions to the chemical shielding of dimethylmercury from the diamagnetic, paramagnetic, and spin–orbit terms. The principal components of the magnetic shielding tensor are given, with the isotropic shielding and the anisotropic components also being listed. These results show that, regardless of the cluster size, the isotropic chemical shielding is approximately 8000 ppm and the span of the chemical shielding tensor is between 7600 and 8000 ppm. The calculations also indicate that the chemical shielding tensor of dimethylmercury is approximately axially symmetric. The diamagnetic contribution is essentially the same for all clusters. The paramagnetic and spin–orbit contributions vary slightly from one cluster to another, but in each case the differences are less than 50 ppm for the paramagnetic contribution and 20 ppm for the spin–orbit contribution. These numbers are close to those of the chemical shielding anisotropy of dimethylmercury reported by Jokisaari et al. particularly for their model C [67]. For the purpose of referencing the chemical shift results, 8000 ppm is used as the isotropic chemical shielding of dimethylmercury.

The results for two clusters representing the local environment of the $HgCl_2$ molecule in the solid are reported in Table 1. The isotropic shifts of the two clusters are approximately 150 ppm less shielding than observed by experiment, consistent with previous calculations using the ZORA–DFT method [66,67]. The calculated spans ($\Omega = |\delta_{33} - \delta_{11}|$) for both clusters are larger than the experimentally measured span. The calculated skews ($\kappa = 3(\delta_{iso} - \delta_{22})/\Omega$) indicate a structure with symmetry very close to axial symmetry [Table 1], a fact that agrees with the X-ray crystallographic point symmetry.

A detailed comparison of the calculated results for the small and large clusters shows some significant differences. All of the elements of the shift tensor for the small cluster are further from the experimental values than are the elements of the large cluster. That being said, the calculated isotropic shifts for the two clusters are virtually identical. This fortuitous agreement results from the fact that the difference between the calculated δ_3 of the two clusters is almost offset by the sum of the opposite deviations of the other elements. While the isotropic shift and the skew are approximately the same for both clusters, the closer agreement of the span with experiment shows that calculations on the large cluster are more consistent with experiment, although these calculations on the large cluster must also be considered qualitative. Thus, the results on the large cluster more accurately represent the local environment in solid $HgCl_2$. This suggests that using the largest clusters possible for calculations is advisable in modeling solid materials.

To understand the state of $HgCl_2$ in solution, one must model interaction between the solvent and the mercury halide. It has been previously suggested that in solutions with solvents like methanol, tetrahydrofuran, DMSO, and pyridine, the degree of association varies from solvent to solvent, and that these interactions affect the observed NMR parameters [14,44–49]. To address the possibility of interactions between $HgCl_2$ and the solvent in DMSO solutions, calculations were performed for a series of clusters that incorporate DMSO with $HgCl_2$ in various geometric configurations (Fig. 10). The results of these calculations are

Table 3
Calculated chemical-shielding parameters of gas-phase dimethylmercury.

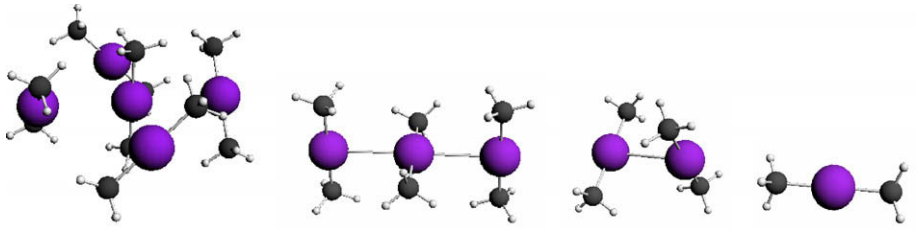

	$\sigma_{P,iso}$ (ppm)	$\sigma_{D,iso}$ (ppm)	$\sigma_{SO,iso}$ (ppm)	$\sigma_{Total,1}$ (ppm)	$\sigma_{Total,2}$ (ppm)	$\sigma_{Total,3}$ (ppm)	$\sigma_{Total,iso}$ (ppm)	Ω (ppm)	κ
Pentamer	−4062	9614	2426	5547	5602	12783	7977	7236	−0.98
Trimer	−4020	9614	2410	5287	5722	13006	8005	7719	−0.89
Dimer	−3966	9614	2448	5466	5692	13128	8095	7663	−0.94
Monomer	−4127	9614	2443	5246	5247	13296	7929	8051	−1.00

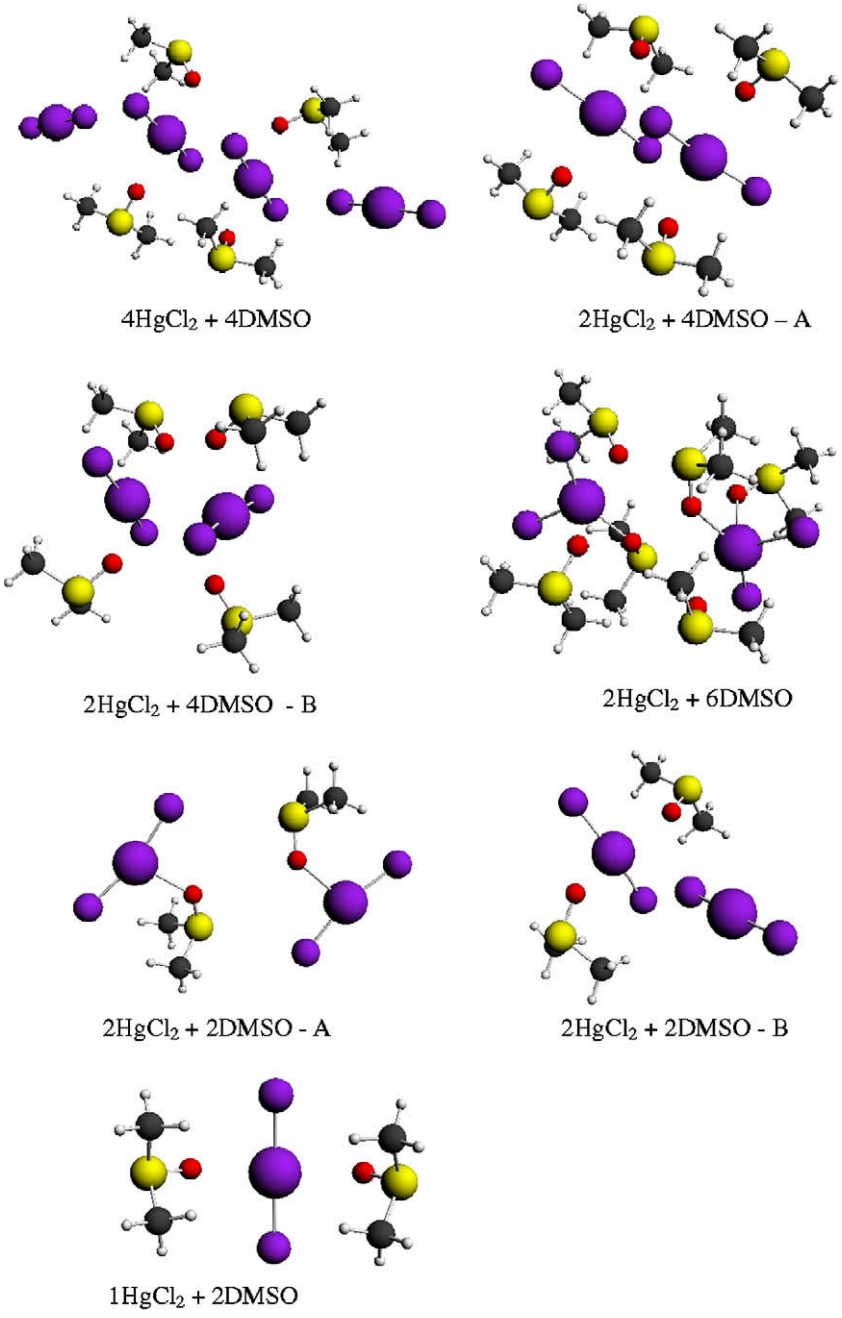

Fig. 10. Model clusters for ZORA–DFT calculations on $HgCl_2$–DMSO structures.

presented in Table 4. In several clusters there are two Hg sites, for each of which the chemical-shielding parameters are reported.

A comparison of the calculated NMR spans of the clusters of $HgCl_2$ with the calculated spans of the two clusters representing $HgCl_2$ in the solid state shows that, in all cases, the calculated spans of the DMSO–$HgCl_2$ complexes are predicted to be smaller than the spans of solid $HgCl_2$, in some instances smaller by a factor of almost 2. This has important implications for the analysis of the experimental relaxation data because the chemical-shielding anisotropy of the complex is what determines the relaxation rate in solution, not the chemical-shielding anisotropy of the pure solid $HgCl_2$. These results are also consistent with the spectrum of the frozen solution in Fig. 6, for which the span is approximately 2300 ppm. Neglecting the cluster of two $HgCl_2$ molecules with six DMSO molecules (for which the span seems much smaller than the others), the spans tend to be around 3000 ppm. For example, the average span over all of these clusters except the last is 3060 ppm. This is in reasonable agreement with the observed span in Fig. 6. The calculated isotropic shifts of the clusters, excepting the last, are in the range from −1645 to −2101 ppm, with an average isotropic shift of −1840 ppm. Again, this is in reasonable agreement with the isotropic shift observed in Fig. 6, considering the state of the art of this kind of calculation. At this level, one cannot distinguish among the various clusters. In fact, in solution the system may exist transiently in each of these environments (and perhaps in even more). What is clear from the calculations and the experiment is that the anisotropy of $HgCl_2$ in solution is smaller than that for $HgCl_2$ in the solid state.

Table 4
Calculated NMR chemical-shift parameters[a] of clusters of $HgCl_2$ and DMSO.

File	δ_{iso} (ppm)	Ω (ppm)	κ
$1HgCl_2$ + 2DMSO	−1907	3160	0.96
$2HgCl_2$ + 2DMSO – A			
(1)	−1698	3596	0.89
(2)	−1663	3600	0.90
$2HgCl_2$ + 2DMSO – B	−1682	3055	0.75
$2HgCl_2$ + 4DMSO – A			
(1)	−1792	2731	0.45
(2)	−2101	2296	0.61
$2HgCl_2$ + 4DMSO – B			
(1)	−1645	3374	0.53
(2)	−2017	2984	0.72
$4HgCl_2$ + 4DMSO			
(1)	−1849	3024	0.63
(2)	−2049	2808	0.69
$2HgCl_2$ + 6DMSO			
(1)	−2264	968	0.43
(2)	−2216	1121	0.61

[a] Calculations assume an isotropic chemical shielding of dimethylmercury of 8000 ppm.

4. Conclusions

The NMR relaxation of $HgCl_2$ in solution in DMSO is shown to be a result of intermolecular and intramolecular interactions, the chemical-shift-anisotropy mechanism being dominant. An estimate of the chemical-shielding anisotropy determined on a frozen solution of $HgCl_2$ in DMSO indicates a rotational correlation time is 69 ps at room temperature. The temperature dependence of the relaxation time constant gives an activation energy for the process modulating the chemical-shift anisotropy of 16.6 ± 1.2 kJ/mol.

Chemical shift measurements on solid $HgCl_2$ at various magnetic-fields and spinning rates define the chemical-shift tensor accurately. In particular, within experimental error, all of the present measurements show that the ^{199}Hg chemical-shift tensor is axially symmetric, in contradiction to an early determination of the chemical-shift tensor of this material [49] by magic-angle spinning. Chemical shift measurements on a frozen solution of $HgCl_2$ in DMSO demonstrate that, when interacting with the solvent, the span of the chemical-shift tensor is reduced to approximately 2270 ppm from the observed solid-state value of 3636 ppm.

ZORA–DFT calculations on clusters that model solid $HgCl_2$ and $HgCl_2$ in DMSO solution predict NMR parameters that are qualitatively in agreement with experiment. That is, the calculations predict that the chemical-shift span of the solid is larger than that of the material in a DMSO solution. However, the results are, at best, qualitative. In particular, the calculations on the various clusters are not sufficient to determine whether one or a few clusters model the situation in solution. In general, the present calculations predict qualitative trends, but the calculated spans are consistently larger than those observed experimentally. The comparison of calculations on two clusters of $HgCl_2$ in the solid state shows that a larger, more extended structure more closely agrees with experiment, but even that agreement is qualitative. This suggests that longer-range effects in the solid state must be considered to get better agreement between theory and experiment.

Acknowledgments

This material is based upon work supported by the National Science Foundation under Equipment Grant # DMR-9975975. CRD acknowledges support of NMR studies by the National Science Foundation under Grant CHE-0411790. The authors thank Barbara Wood for measurement of viscosities.

Appendix A. Supplementary data

Supplementary data associated with this article can be found, in the online version, at doi:10.1016/j.molstruc.2009.04.045.

References

[1] Wikipedia http://en.wikipedia.org/wiki/Main_Page, "Qin Shi Huang" and "Mad Hatter", 2008 (accessed 10.10.08).
[2] P. Atkins, L. Jones, Chemical Principles – The Quest for Insight, W.H. Freeman and Company, New York, 1999 (p. 761).
[3] W.G. Proctor, F.C. Yu, Phys. Rev. 81 (1951) 20–30.
[4] B. Wrackmeyer, R. Contreras, ^{199}Hg NMR parameters, in: G. Webb, I. Ando (Eds.), Annual Reports on NMR Spectroscopy, vol. 24, Elsevier, 1992, pp. 267–329.
[5] C.R. Lassigne, E.J. Wells, Can. J. Chem. 55 (1977) 1303–1313.
[6] R.E. Wasylishen, R.E. Lenkinski, C. Rodger, Can. J. Chem. 60 (1982) 2113–2117.
[7] M. Maliarik, I. Persson, Magn. Reson. Chem. 43 (2005) 835–842.
[8] G.E. Maciel, M. Borzo, J. Magn. Reson. 10 (1973) 388–390.
[9] M.A. Sens, N.K. Wilson, P.D. Ellis, J.D. Odom, J. Magn. Reson. 19 (1975) 323–336.
[10] M.C. Day Jr., J. Selbin, Theoretical Inorganic Chemistry, Reinhold Book Corp., New York, 1969 (p. 376).
[11] P. Peringer, Inorg. Chim. Acta 39 (1980) 67–70.
[12] M. Sandström, I. Persson, P. Persson, Acta Chem. Scand. 44 (1990) 653–675.
[13] V. Subramanian, K. Seff, Acta Cryst. B 36 (1980) 2132–2135.
[14] I. Persson, M. Sandström, P.L. Goggin, Inorg. Chim. Acta 129 (1987) 183–197.
[15] R.K. Harris, A. Sebald, Magn. Reson. Chem. 25 (1987) 1058–1062.
[16] M.J. Natan, C.F. Millikan, J.G. Wright, T.V. O'Halloran, J. Am. Chem. Soc. 112 (1990) 3255–3257.
[17] R.A. Santos, E.S. Gruff, S.A. Koch, G.S. Harbison, J. Am. Chem. Soc. 113 (1991) 469–475.
[18] C.J. Groombridge, Magn. Reson. Chem. 31 (1993) 380–387.
[19] K. Eichele, S. Kroeker, G. Wu, R.E. Wasylishen, Solid State NMR 4 (1995) 295–300.
[20] J.M. Hook, P.A.W. Dean, L.C.M. van Gorkom, Magn. Reson. Chem. 33 (1995) 77–79.
[21] T.C. Farrar, E.D. Becker, Pulse and Fourier Transform NMR, Introduction to Theory and Methods, Academic Press, New York, 1971 (pp. 20–22).
[22] A.L. Van Geet, Anal. Chem. 40 (1968) 2227–2229.
[23] P.A. Beckman, C. Dybowski, J. Magn. Reson. 146 (2000) 379–380.
[24] A. Bielecki, D.P. Burum, J. Magn. Reson. A 116 (1995) 215–220.
[25] G. Neue, C. Dybowski, Solid State NMR 7 (1997) 333–336.
[26] R.E. Taylor, Concepts Magn. Reson. A 22 (2004) 79–89.
[27] E.J. Baerends, J. Autschbach, A. Bérces, F.M. Bickelhaupt, C. Bo, P.L. de Boeij, P.M. Boerrigter, L. Cavallo, D.P. Chong, L. Deng, R.M. Dickson, D.E. Ellis, L. Fan, T.H. Fischer, C. Fonseca Guerra, S.J.A. van Gisbergen, J.A. Groeneveld, O.V. Gritsenko, M. Grüning, F.E. Harris, P. van den Hoek, C.R. Jacob, H. Jacobsen, L. Jensen, G. van Kessel, F. Kootstra, E. van Lenthe, D.A. McCormack, A. Michalak, J. Neugebauer, V.P. Osinga, S. Patchkovskii, P.H.T. Philipsen, D. Post, C.C. Pye, W. Ravenek, P. Ros, P.R.T. Schipper, G. Schreckenbach, J.G. Snijders, M. Solà, M. Swart, D. Swerhone, G. te Velde, P. Vernooijs, L. Versluis, L. Visscher, O. Visser, F. Wang, T.A. Wesolowski, E. van Wezenbeek, G. Wiesenekker, S.K. Wolff, T.K. Woo, A.L. Yakovlev, T. Ziegler, Amsterdam Density Functional Program (ADF), 2006.01.
[28] G. Schreckenbach, T. Ziegler, J. Phys. Chem. 99 (1995) 606–611.
[29] G. Schreckenbach, T. Ziegler, Int. J. Quantum Chem. 60 (1996) 753–766.
[30] G. Schreckenbach, T. Ziegler, Int. J. Quantum Chem. 61 (1997) 899–918.
[31] S.K. Wolff, T. Ziegler, J. Chem. Phys. 109 (1998) 895–905.
[32] S.H. Vosko, L. Wilk, M. Nusair, Can. J. Phys. 58 (1980) 1200–1211.
[33] A.D. Becke, Phys. Rev. A 38 (1988) 3098–3100.
[34] J.P. Perdew, Phys. Rev. B 33 (1986) 8822–8824.
[35] The Inorganic Crystal Structure Database is copyrighted by the Fachinforationszentrum Karlsruhe and the National Institute of Standards and Technology, Information on the database is available at http://icsdweb.fizkarlsruhe.de/.
[36] C.C. Pye, T. Ziegler, Theor. Chem. Acc. 101 (1999) 396–408.
[37] A. Klamt, G. Schüürmann, J. Chem. Soc. Perkin Trans. 2 (1993) 799–805.
[38] A. Klamt, J. Phys. Chem. 99 (1995) 2224–2235.
[39] A. Klamt, V. Jones, J. Chem. Phys. 105 (1996) 9972–9981.
[40] F.A. Cotton, R. Francis, J. Am. Chem. Soc. 82 (1960) 2986–2991.
[41] J. Selbin, W.E. Bull, L.H. Holmes Jr., J. Inorg. Nucl. Chem. 16 (1961) 219–224.
[42] P. Biscarini, L. Fusina, G.D. Nivellini, J. Chem. Soc. A (1971) 1128–1131.
[43] P. Biscarini, L. Fusina, G.D. Nivellini, A. Mangia, G. Pelizzi, J.C.S. Dalton 17 (1974) 1846–1849.
[44] R. Fraginals, N. Barba-Behrens, R. Contreras, Spectrochim. Acta 45A (1989) 581–584.
[45] J.P. Joly, I.F. Nicolau, Spectrochim. Acta 35A (1979) 281–289.
[46] M. Sandström, Acta Chem. Scand. Ser. A 32 (1978) 627–641.
[47] J. Herzfeld, A.E. Berger, J. Chem. Phys. 73 (1980) 6021–6030.

[48] Y.K. Grishin, D.V. Bazhenov, Y.A. Ustynyuk, V.M. Mastikhin, J. Struct. Chem. 28 (1987) 850–853.
[49] G.A. Bowmaker, A.V. Churakov, R.K. Harris, S.-W. Oh, J. Organomet. Chem. 550 (1998) 89–99.
[50] D. Massiot, I. Farnan, N. Gautier, D. Trumeau, A. Trokiner, J.P. Coutures, Solid State NMR 4 (1995) 241–248.
[51] R.K. Harris, E.D. Becker, S.M.C. De Menezes, P. Granger, R.E. Hoffman, K.W. Zilm, Solid State NMR 33 (2008) 41–56.
[52] P.W. Atkins, Physical Chemistry, W.H. Freeman and Company, San Francisco, 1978. p. 843.
[53] D.G. Gillies, L.P. Blaauw, G.R. Hays, R. Huis, A.D.H. Clague, J. Magn. Reson. 42 (1981) 420–428.
[54] A. Bondi, J. Phys. Chem. 68 (1964) 441–451.
[55] D. Kivelson, S.J.K. Jensen, M.-K. Ahn, J. Chem. Phys. 58 (1973) 428–433.
[56] M.G. Kurnikova, N. Balabai, D.H. Waldeck, R.D. Coalson, J. Am. Chem. Soc. 120 (1998) 6121–6130.
[57] J.L. Dote, D. Kivelson, R.N. Schwartz, J. Phys. Chem. 85 (1981) 2169–2180.
[58] A. Abragam, Principles of Nuclear Magnetism, Clarendon Press, Oxford, 1961 (p. 316).
[59] D.F. Shriver, P.W. Atkins, Inorganic Chemistry, third ed., W.H. Freeman and Company, New York, 1999 (p. 468).
[60] J.E. Huheey, E.A. Keiter, R.L. Keiter, Inorganic Chemistry – Principles of Structure and Reactivity, fourth ed., Harper Collins College Publishers, New York, 1993 (pp. 548–549).
[61] L.E. Reichl, A Modern Course in Statistical Physics, University of Texas Press, Austin, Tx, 1980 (Chapter 13).
[62] M. Holz, S.R. Heil, A. Sacco, Phys. Chem. Chem. Phys. 2 (2000) 4740–4742.
[63] C.B. Harris, D.E. Smith, D.J. Russell, Chem. Rev. 90 (1990) 481–488.
[64] N. Balabai, A. Sukharevsky, I. Read, B. Strazisar, M. Kurnikova, R.S. Hartman, R.D. Coalson, D.H. Waldeck, J. Molecular, Liquids 77 (1998) 37–60.
[65] H. Nakatsuji, M. Hada, H. Kaneko, C.C. Ballard, Chem. Phys. Lett. 255 (1996) 195–202.
[66] S.K. Wolff, T. Ziegler, E. van Lenthe, E.J. Baerends, J. Chem. Phys. 110 (1999) 7689–7698.
[67] J. Jokisaari, S. Järvinen, J. Autschbach, T. Ziegler, J. Phys, Chem. A 106 (2002) 9313–9318.
[68] J. Autschbach, A.M. Kantola, J. Jokkisaari, J. Phys. Chem. A 111 (2007) 5343–5348.
[69] J. Autschbach, T. Ziegler, J. Am. Chem. Soc. 123 (2001) 3341–3349.